

Supplement of The Cryosphere, 13, 2579–2595, 2019
<https://doi.org/10.5194/tc-13-2579-2019-supplement>
© Author(s) 2019. This work is distributed under
the Creative Commons Attribution 4.0 License.



Supplement of

Spatial and temporal variations in basal melting at Nivlisen ice shelf, East Antarctica, derived from phase-sensitive radars

Katrin Lindbäck et al.

Correspondence to: Katrin Lindbäck (katrin.lindback@npolar.no)

The copyright of individual parts of the supplement might differ from the CC BY 4.0 License.

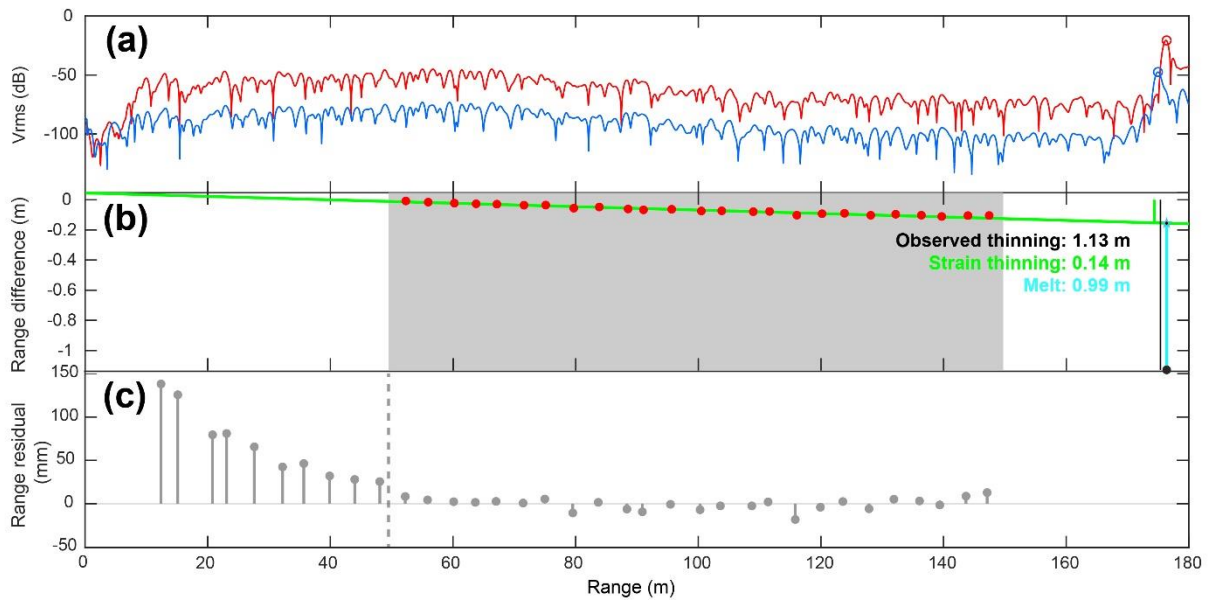


Figure S1. Calculation of basal melt from ApRES at the seaward overwintering site (Fig. 1b): **(a)** Fourier transform of mean chirps from first (red) and second (blue) visit after aligning to account for snow accumulation. Basal displacement was calculated by cross-correlating the portion of the returns around the basal maxima (red and blue circles). For FMCW radar, the frequency of each component of the data that are acquired represents the range to a reflector via the formula $R = T \cdot f \cdot v_i / (2 \cdot B)$, where v_i is the radar speed in ice, f is the frequency associated with the reflection at range R , T is the length of the chirp in seconds, and B is the bandwidth of the chirp. **(b)** Estimating vertical strain using linear fit (green line) of relative internal layer motion (red dots). Grey box is the depth window for the strain estimation. The given rate for observed thinning is the sum of basal melt rate and strain thinning, assuming a uniform strain rate through the thickness column below the firn layer. **(c)** Firm depth (dashed vertical line) extracted as a deviation from the strain line fit.

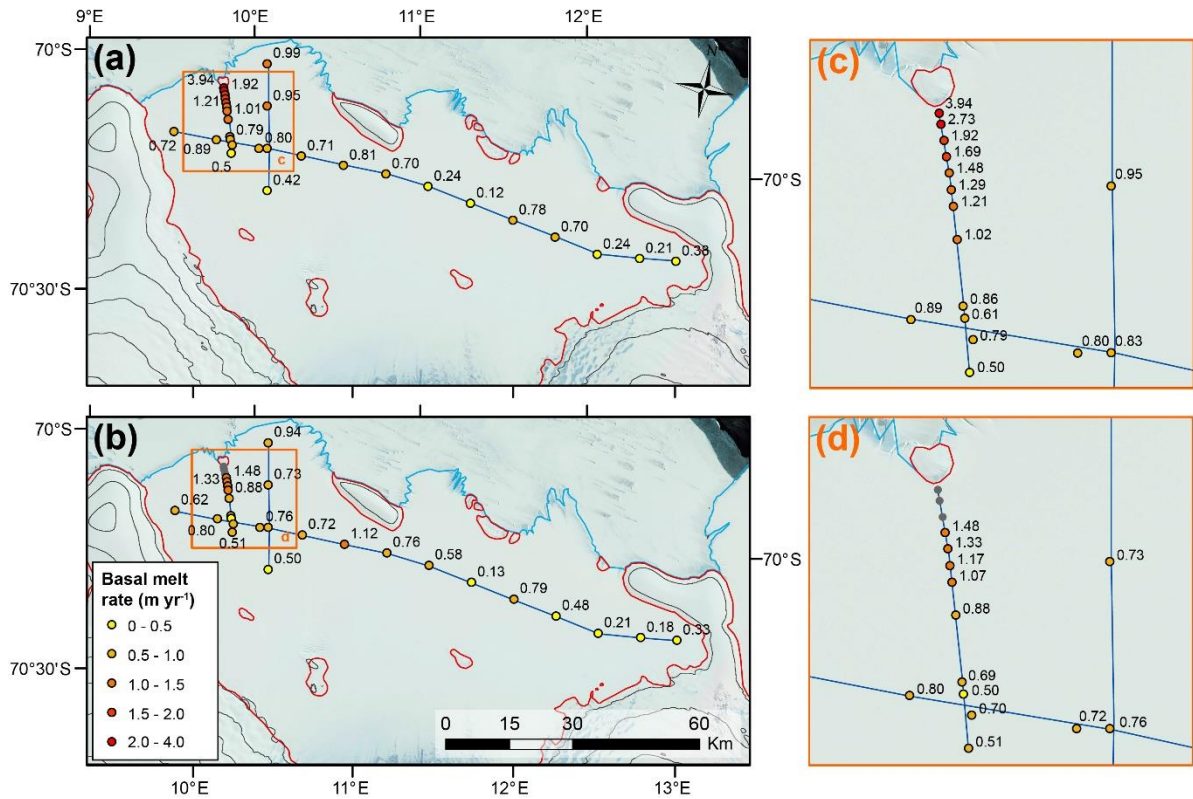


Figure S2. Annual averaged basal melt rates derived from ApRES in (a) 2017 and (b) 2018. (c) and (d) shows the melt rates towards an ice rump. Three locations closest to the rump were not reoccupied in Dec 2018. Contour lines and background images are the same as in Fig. 1 of the main paper. Basal melt rates were slightly lower in the second year at 18 sites and for 8 sites slightly higher.

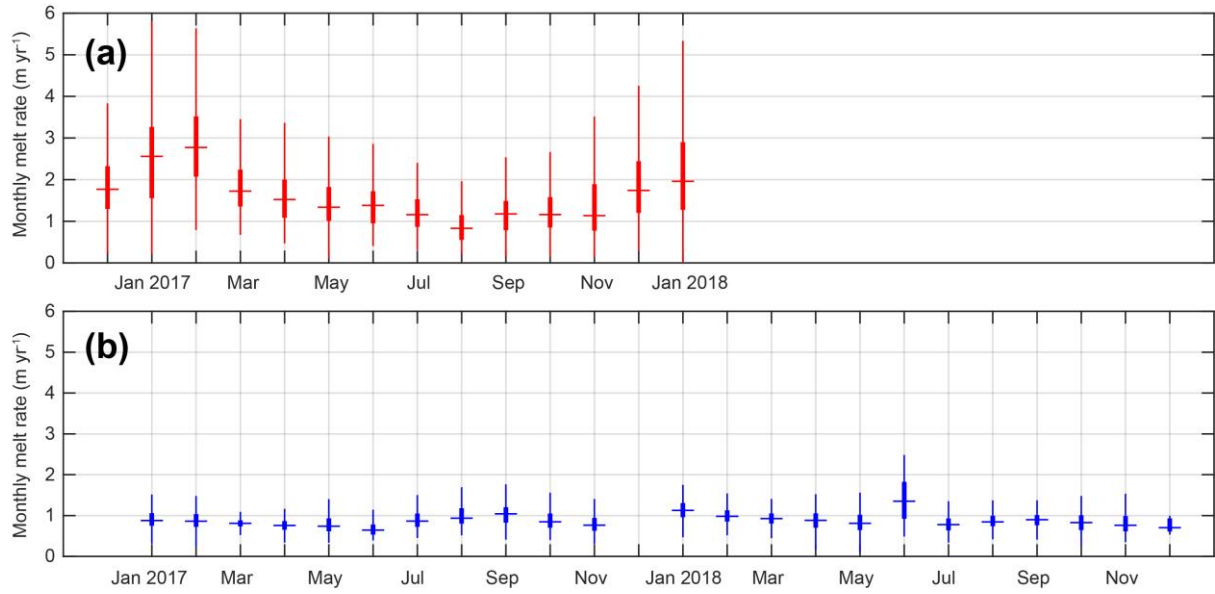


Figure S3. Box plots of basal melting for every month from Dec 2016–Dec 2018 at the **(a)** seaward and **(b)** landward site. On each box, the central mark is the median basal melt, the edges of the box are the twenty-fifth and seventy-fifth percentiles, and the whiskers extend to the most extreme basal melt measurements during a month that are not considered to be outliers.

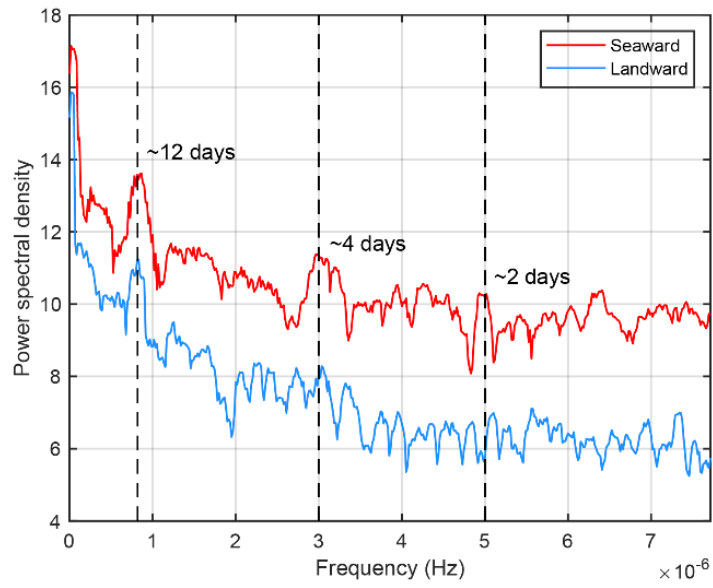


Figure S4. Power spectral density estimates of the normalized 36 h filtered seaward and landward basal melt rates.

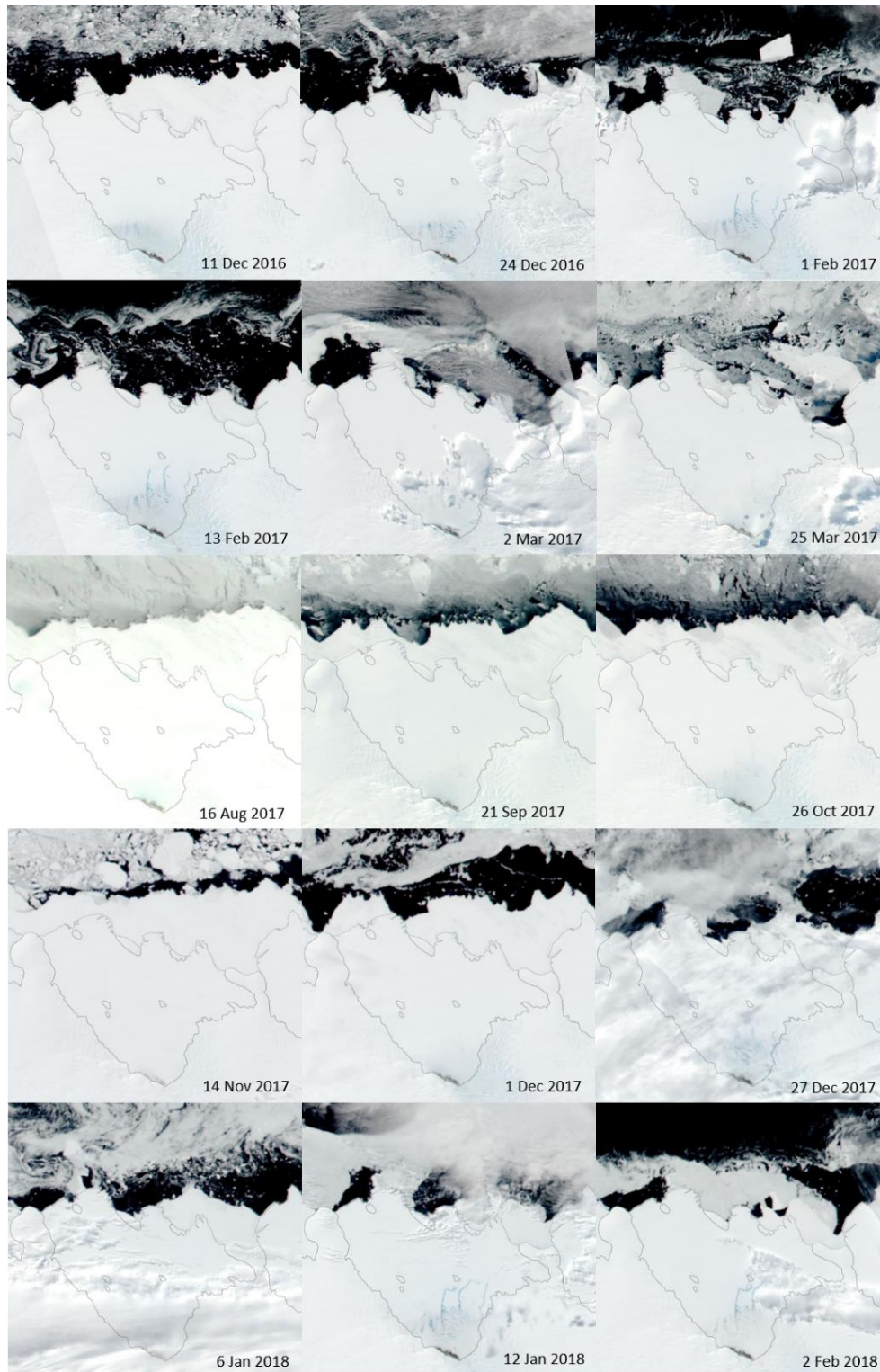


Figure S5. MODIS corrected reflectance imagery from NASA Worldview showing the main developments in sea ice cover in front of Nivlisen during the observational period of the seaward ApRES station (11 Dec 2016–4 Feb 2018). Sea ice is widespread in front of Nivlisen during winter and then partly breaks up during summer, typically starting from the west and progressing to the more sheltered eastern side. The general pattern of summer retreat is interrupted by irregular periods of sea ice re-growth (e.g. early February 2017 and 2018).